Bulletin of the Seismological Society of America, Vol. 85, No. 1, pp. 66–82, February 1995

Liquefaction during the 1990 Manjil, Iran, Earthquake, I: Case History Data

by M. K. Yegian, V. G. Ghahraman, M. A. A. Nogole-Sadat, and H. Daraie

Abstract During the 1990 Manjil, Iran, earthquake (M_S = 7.7), an estimated 35,000 people lost their lives and more than 300,000 were left homeless. The earthquake ground shaking caused enormous destruction of unreinforced structures. In addition, widespread liquefaction contributed significantly to building damage in towns as far away as 85 km from the ruptured fault. Following the earthquake, the authors surveyed the liquefaction regions, conducted geotechnical field explorations, and documented case histories on liquefaction of level ground, liquefaction-induced building settlement, permanent ground displacement, and performance of piles and piers in liquefied soils. This article presents and discusses the data of the case histories investigated. In addition, based on the evidence from the Manjil earthquake, the importance of geologic input in mapping of liquefaction potential in earthquake-prone regions is demonstrated. In the companion article, the authors present the results of their analyses of liquefaction-related case histories.

Introduction

On 21 June 1990, shortly after midnight, an earthquake of surface-wave magnitude M_S = 7.7 struck the northwestern region of Iran. More than 35,000 people lost their lives and about 300,000 people were left homeless. Within the earthquake-damage zone, which is primarily rural, the earthquake ground shaking caused heavy damage to one- and two-story unreinforced brick and masonry structures. Liquefaction of foundation soils also contributed significantly to the destruction of many residential, commercial, and public buildings. Evidence of widespread liquefaction-induced damage could be observed as far away as 85 km from the ruptured fault.

Following the earthquake, a number of engineers, geologists, and seismologists from Iran as well as from the United States, China, and Japan surveyed the damage zone. Preliminary reports and technical articles on the various aspects of the earthquake have been prepared by Moinfar and Naderzadeh (1990), Astaneh and Ghafori-Ashtiany (1990), Yegian and Ghahraman (1990), Raifa *et al.* (1990), Mehrain (1990), Peng and Mozaffari (1990), Ishihara *et al.* (1992), Berberian *et al.* (1992), Niazi and Bozorgnia (1992), Haeri and Zolfaghari (1992), and Shoaei and Sassa (1993). From the preliminary assessments, it was evident that liquefaction-induced damage was an important aspect that warranted further investigation.

With support from the Ministry of Housing and Urban Development of the government of Iran, and the Office of the Governor of the Guilan Province, the authors conducted an extensive investigation of the liquefaction-related aspects of the earthquake. Field surveys and geotechnical investigations were performed to obtain relevant site and structural data to document and analyze liquefaction case histories.

This article presents an overview of the earthquake and liquefaction-induced damage as well as the case history data that the authors have compiled. In the companion article (Yegian *et al.*, 1995), the authors present the results of their analyses of the ground motions, and of the case histories on liquefaction of level ground, permanent ground deformation, and liquefaction-induced settlement of buildings.

The Earthquake

The surface magnitude of the 21 June 1990 earthquake was estimated to be 7.7 (Berberian *et al.*, 1992). The epicenter of the earthquake was inferred to be at or near the town of Manjil, located 180 km northwest of the capital, Tehran (Fig. 1). The earthquake generated a right-lateral thrust fault with an effective length of about 80 km, as shown in Figure 2 (Berberian *et al.*, 1992). Within a region of 200 km from the fault, a number of strong-motion accelerograms recorded the ground motions. In Figure 2, the locations of selected cities and towns, and values of the recorded peak ground accelerations, are shown. Table 1 presents the complete list

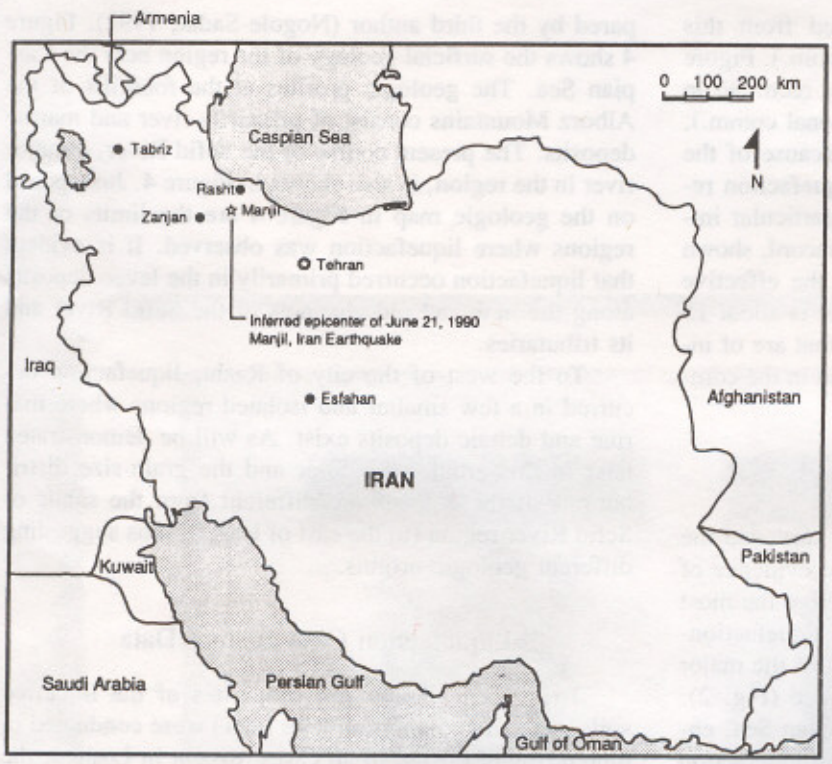

Figure 1. Location of the inferred epicenter of the 21 June 1990 Manjil, Iran, earthquake.

Figure 2. Selected locations where peak ground accelerations were recorded, and regions of liquefaction.

of the peak ground accelerations obtained from this earthquake (Naderzadeh, 1991, personal comm.). Figure 3 shows a typical acceleration time history recorded in the city of Lahijan (Naderzadeh, 1991, personal comm.), which is located 62 km from the fault. Because of the proximity of Lahijan to the widespread liquefaction region shown in Figure 2, this record is of particular importance. Although the total duration of this record, shown in Figure 3, appears to be about 60 sec, the effective duration of interest for liquefaction analysis is about 15 sec. Further characteristics of this record, that are of interest for liquefaction analysis, are discussed in the companion article.

Liquefaction Regions

Following the earthquake, the authors surveyed the damage zone to document and evaluate the evidence of liquefaction. From this survey it was clear that the most widespread occurrence of liquefaction and liquefaction-induced damage was in a region to the east of the major city of Rasht, capital of the Guilan province (Fig. 2). This region, which is located near the Caspian Sea, encompasses the town of Astaneh-Ashrafieh. Liquefaction was also observed, although to a lesser extent, in small regions west of Rasht, the most significant of which occurred in and near the town of Leef-Shagerd (Fig. 2). Also, in Loshan, 15 km from the fault (Fig. 2), extensive evidence of liquefaction was observed. At this site, the performance of bridge piers and pile foundations in liquefied sands was investigated.

To understand why liquefaction was so widespread, yet confined to distinct regions, especially near the Caspian Sea, a detailed geologic map of the area was prepared by the third author (Nogole-Sadat, 1992). Figure 4 shows the surficial geology of the region near the Caspian Sea. The geologic profiles at the foothills of the Alborz Mountains consist of primarily river and marine deposits. The present course of the Sefid River, a major river in the region, is also shown in Figure 4. Juxtaposed on the geologic map in Figure 4 are the limits of the regions where liquefaction was observed. It is evident that liquefaction occurred primarily in the levee deposits along the new and old channels of the Sefid River and its tributaries.

To the west of the city of Rasht, liquefaction occurred in a few smaller and isolated regions where marine and deltaic deposits exist. As will be demonstrated later in this article, the color and the grain-size distributions of these sands are different from the sands of Sefid River region (to the east of Rasht), thus suggesting different geologic origins.

Table 1
Recorded Peak Ground Accelerations from the 1990 Manjil, Iran, Earthquake (Naderzadeh, 1991, personal comm.)

Location	Distance from the Fault (km)	Peak Ground Acceleration pga(g)		
		L Comp.	*T* Comp.	*V* Comp.
Ab-bar	7	0.55	0.52	0.56
Ghazvin	50	0.19	0.13	0.09
Lahijan	62	0.12	0.18	0.09
Zanjan	70	0.10	0.06	0.06
Roudsar	70	0.10	0.08	0.07
Abhar	73	0.13	0.20	0.07
Tonkabon	100	0.13	0.09	0.03
Eshtehard	115	0.06	0.07	0.05
Mianeh	135	0.02	0.02	—
Ardebil	140	0.02	0.09	0.02
Karaj	140	0.04	0.02	0.03
Gachsar	150	0.06	0.10	0.03
Robat-Kareem	170	0.04	0.05	0.02
Kahrizak	190	0.03	0.02	0.02
Roud-e-Shour	215	0.03	0.03	0.01

Liquefaction Case History Data

To evaluate the *in situ* properties of the liquefied soils, standard penetration tests (SPT) were conducted in nine different towns. In all cases, except in Loshan, the SPT tests were performed using a standard 2-inch split-spoon sampler without a liner. The energy transfer mechanism consisted of a safety hammer with two wraps of a rope around a pulley. Drilling mud was used to prevent caving of the boreholes, especially below the water table. In Loshan, because of inaccessibility of the sites, a hand cone penetrometer was used for shallow investigations. Based on SPT and cone penetration test results performed on similar sands in the region, the equivalent field SPT values for the sands in Loshan were estimated.

The number of boreholes made in each town depended on the level and extent of liquefaction-induced damage. Figure 5 shows a map of the region near the Caspian Sea where liquefaction-induced damage was widespread. As stated earlier, to the east of Rasht, liquefaction occurred almost entirely in the levee deposits along the banks of the Sefid and Heshmat rivers, as shown in Figure 5. To the west of Rasht, liquefaction was ob-

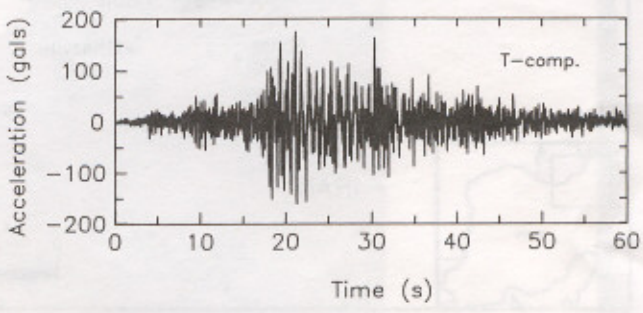

Figure 3. The transverse component of the acceleration time history recorded in Lahijan.

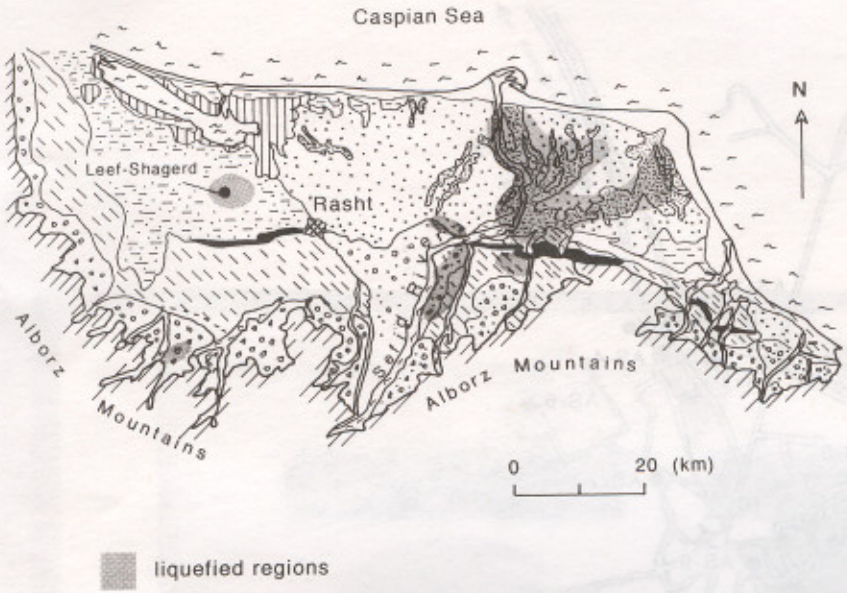

Figure 4. Map of surficial geology of the region near the Caspian Sea, and regions of liquefaction.

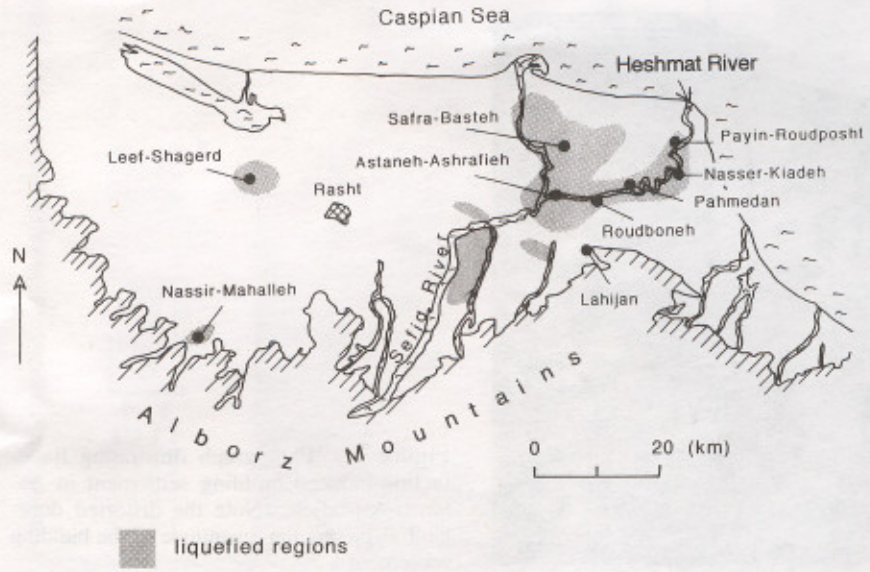

Figure 5. Location of towns where geotechnical field investigations were conducted.

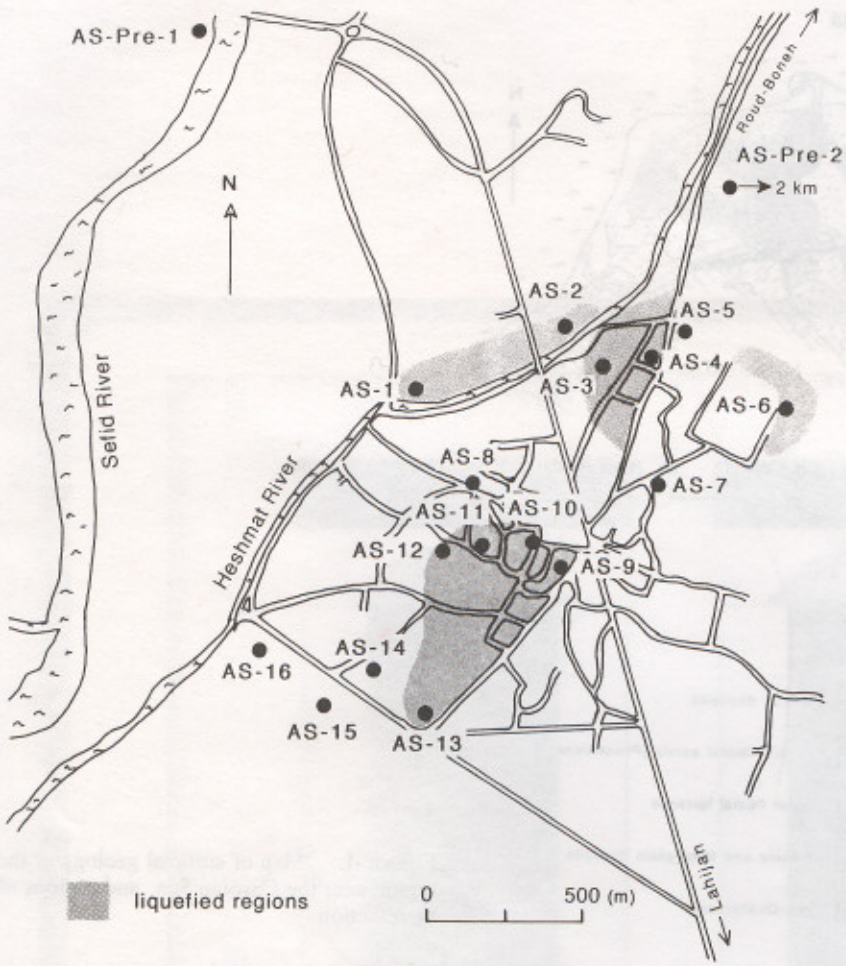

Figure 6. Location of boreholes and regions of liquefaction in the town of Astaneh-Ashrafieh.

Figure 7. Photograph illustrating liquefaction-induced building settlement in Astaneh-Ashrafieh. (Note the distorted doorjamb depicting the magnitude of the building settlement.)

Figure 8. Liquefaction-induced settlement (70 cm) of a two-story building in Astaneh-Ashrafieh.

served in and near the towns of Leef-Shagerd and Nassir-Mahalleh. Because of the differences in the geologic origins of the liquefied sands in the three regions identified in Figure 2 (namely, east of Rasht, west of Rasht, and Loshan regions), the field investigation results are presented separately for each region.

Data East of Rasht

The most dramatic evidence of liquefaction from the Manjil earthquake was observed in this region, and particularly in the major town of Astaneh-Ashrafieh. Figure 6 shows a town map and the regions where liquefaction was evident. The town is located almost entirely on the south bank of the Heshmat River, a major tributary of the Sefid River. In this town, one- and two-story structures experienced liquefaction-induced settlements as large as 70 cm (Figs. 7 and 8). Also, in numerous places, sand boils were formed and water wells were filled with liquefied sands (Fig. 9). As shown in Figure 6, in the town of Astaneh-Ashrafieh, liquefaction occurred only in certain sections of the town. To understand the reason behind this, standard penetration tests were performed in 16 boreholes, distributed over the entire town, including sections where liquefaction was not observed, as shown in Figure 6. Figure 10 presents the borehole logs from the liquefied zones in Astaneh-Ashrafieh. It is noted that these field borings were made in the summer of 1991, almost exactly a year after the earthquake. Although during the time of our field investigations the water table was generally about 4 m below ground surface, it has been reported that at the time of the earthquake the water level in the wells was only about 2 m below ground sur-

Figure 9. A water well in Astaneh-Ashrafieh filled with rising liquefied sand.

face. This is mainly due to seasonal changes in the water regime of the region. For interpreting the *in situ* field data, the water table elevation recorded during the field investigation (4 m below ground) was used. However, for analyses of observed liquefaction case histories, the water table at the time of the earthquake (2 m below ground) was used. Figure 10 also shows the range of the grain-size distribution of the sands retrieved from the boreholes. The liquefied sands from these boreholes are grey, uniform, fine grained, and have less than 12% silt. Figure 11 shows the borehole logs from areas in Astaneh-Ashrafieh where there was no evidence of liquefaction. The range of grain-size distribution of the sands encountered in these boreholes is very similar to that of the sands from the liquefied zones. This is not surprising, since the sands in Astaneh-Ashrafieh have the same geologic origin. A visual comparison between the SPT results of the liquefied and nonliquefied sands shows that, as expected, in general the liquefied sands are looser.

It is of interest to compare the SPT values obtained after the earthquake with those recorded prior to the earthquake. The locations of two preearthquake boreholes are shown in Figure 6. Although these boreholes are not within the city of Astaneh-Ashrafieh, and considering the fact that subsurface conditions may very even within short distances, they are close enough to be used for qualitative comparison. Figure 12 shows the logs of these two preearthquake boreholes. It is evident that the SPT values prior to the earthquake for the sands in Astaneh-Ashrafieh, especially for the depth between 5 and

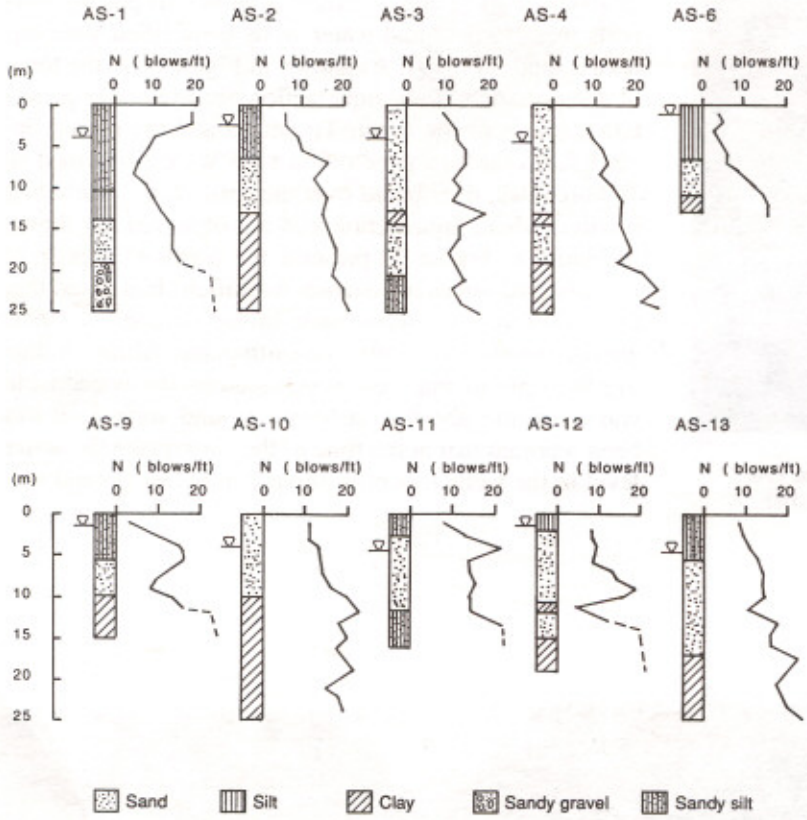

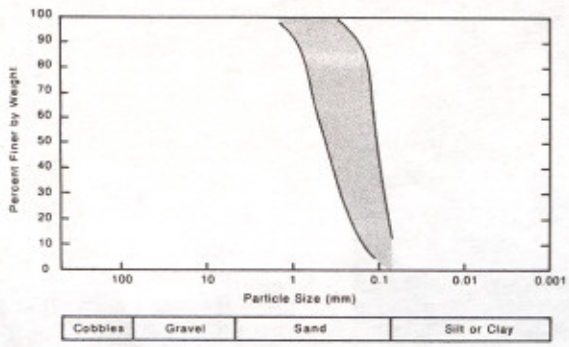

Figure 10. Borehole logs from liquefied sands in Astaneh-Ashrafieh, and range of grain-size distribution.

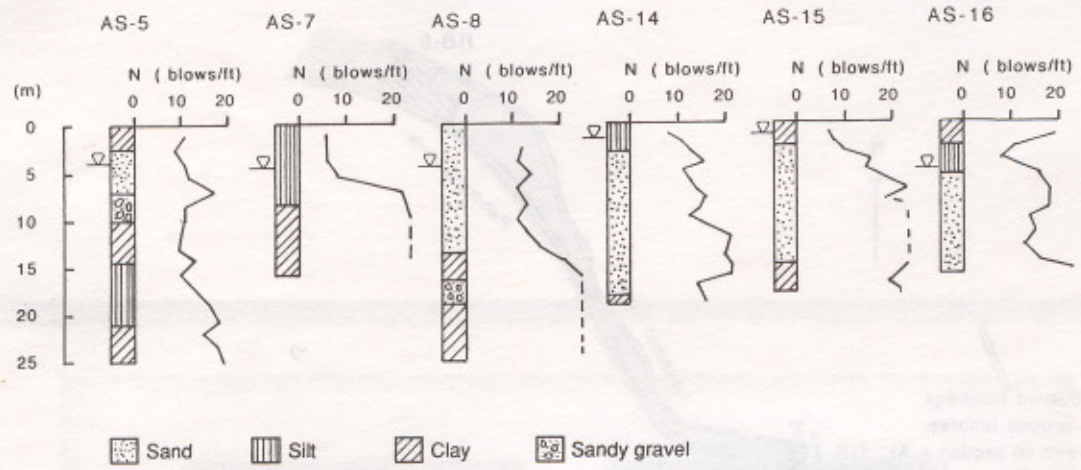

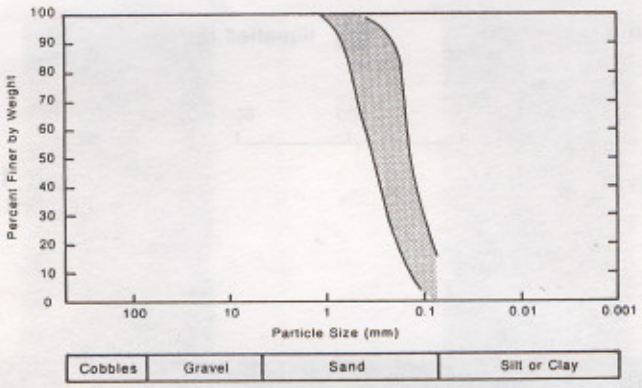

Figure 11. Borehole logs from nonliquefied sands in Astaneh-Ashrafieh, and range of grain-size distribution.

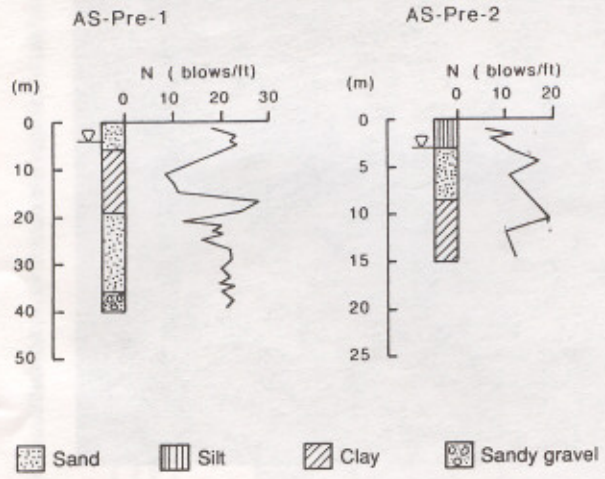

Figure 12. Preearthquake borehole logs from Astaneh-Ashrafieh.

10 m, are similar to those obtained after the earthquake (between 10 and 20 blows/ft).

In the town of Roudboneh, 5 km east of Astaneh-Ashrafieh (Fig. 5), the liquefaction-induced damage was extensive. Figure 13 shows a map of Roudboneh and the liquefied region along the Heshmat River. Evidence of liquefaction was abundant in the form of sand boils, sand-filled water wells, building settlements, settlement and cracking of the roadway, and permanent displacements of the ground toward the Heshmat River. In the companion article, the geotechnical profile along A-A (shown in Fig. 13) is presented and analyzed for settlements and permanent displacements. Figure 14 shows a photograph of a school playground that was flooded with ejected sand and water. A row of stores that experienced settlement of about 60 to 70 cm is shown in Figure 15. In Roudboneh, five boreholes were made and their locations are

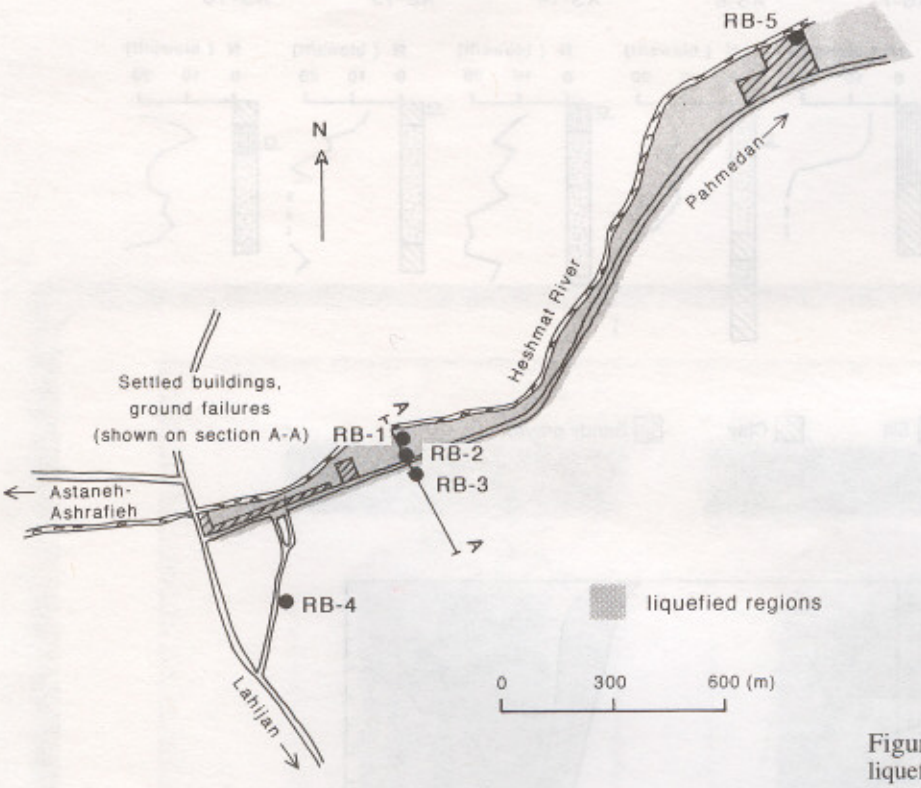

Figure 13. Location of boreholes, and liquefied region in Roudboneh.

Figure 14. Photograph of a school yard in Roudboneh covered with ejected liquefied sand and water.

shown in Figure 13. The borehole logs and the range of grain-size distribution of the sands from these boreholes are presented in Figure 16. It is evident that in Roudboneh, sands susceptible to liquefaction are present mainly between the roadway and the Heshmat River.

In other towns and villages located to the east of Rasht, although liquefaction was widespread, the extent of damage to structures was lower because of the lower population densities (compared to Astaneh-Ashrafieh and Roudboneh). Limited field investigations were made in four additional towns, the locations of which are shown in Figure 2. The borehole logs from Pahmedan are shown in Figure 17 and those from Payin-Roudposht, Nasser-Kiadeh, and Safra-Basteh in Figure 18. These boreholes were made adjacent to one- and two-story structures that experienced liquefaction-induced settlements. In the companion article, the SPT results from these locations are used in analyses of liquefaction and building settlement.

It is noted that the color and grain-size distribution of the liquefied sands investigated from all locations east of Rasht (Figs. 16, through 18) are very similar, suggesting that these sands may have the same geologic origin, as also shown in the surficial geologic map of Figure 4.

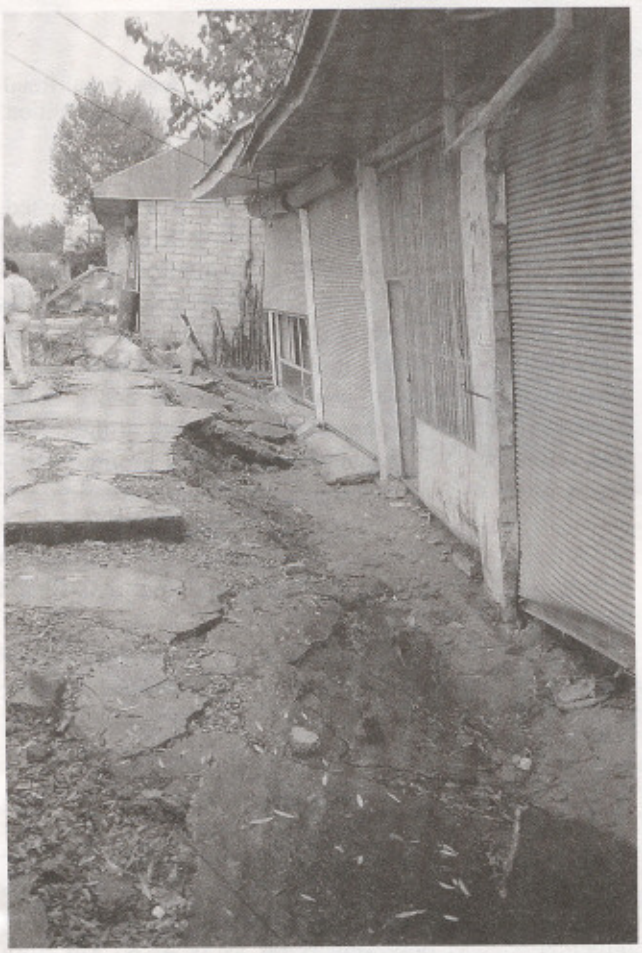

Figure 15. Photograph depicting liquefaction-induced settlement (60 to 70 cm) of a row of stores in Roudboneh.

Data West of Rasht

Liquefaction was also observed in a number of isolated locations to the west of Rasht. Field investigations were made in Leef-Shagerd and in Nassir-Mahalleh, the locations of which are shown in Figure 5. Figure 19 shows the SPT results from these two small towns. It is of interest to note that the sands from these two locations, unlike the sands encountered to the east of Rasht, are well graded and brown in color.

Data near Loshan

Near the outskirts of the town of Loshan, 15 km south of the ruptured fault, evidence of liquefaction was observed along the banks of the Shahroud River, which is another tributary of the Sefid River. Of particular significance were the observations made near and around the Bala-Bala bridge, which is part of a major highway that connects the capital, Tehran, to Rasht. Figure 20 shows a close-up map of the Bala-Bala region and the location of two cross sections A-A and B-B that were investigated. The profile along section A-A, together with the various observations made, is shown in Figure 21. Adjacent to the Shahroud River, numerous sand boils were found (Fig. 22). Also, there was evidence of liquefaction-induced flow slide from the location of the bridge toward the river (Fig. 23). Around the bridge piers, ground settlements of up to 40 cm and lateral soil movement of up to 50 cm were measured (Fig. 24). In addition, adjacent to the bridge, a 6-m-high dike suffered settlement cracks (Fig. 20), and there was evidence of sand ejected near the toes. Amidst all this widespread liquefaction, the bridge sustained neither any damage nor measurable settlements and distortions. Figure 25 shows details of the bridge and its foundation piers. Because of the difficult and inaccessible terrain, standard penetration tests could not be performed at this site. A hand cone penetrometer was utilized and the penetration resistances of the soils down to a depth of 2 m were measured. These values were then correlated to SPT results from Roudboneh by repeating the cone tests in Roudboneh as described earlier. Based on this, an approximate value of field SPT of 12 blows/ft was estimated for the sands in Bala-Bala. The grain-size distribution shown in Figure 26 indicates that the sands in Bala-Bala are very similar to those found along the banks of Sefid River to the east of Rasht. The thickness of the sand deposit was also approximated based on boreholes previously made near the river, about 100 to 200 m from this site. These boreholes were made, unfortunately, without SPT.

Also, near the Bala-Bala bridge, the performance of

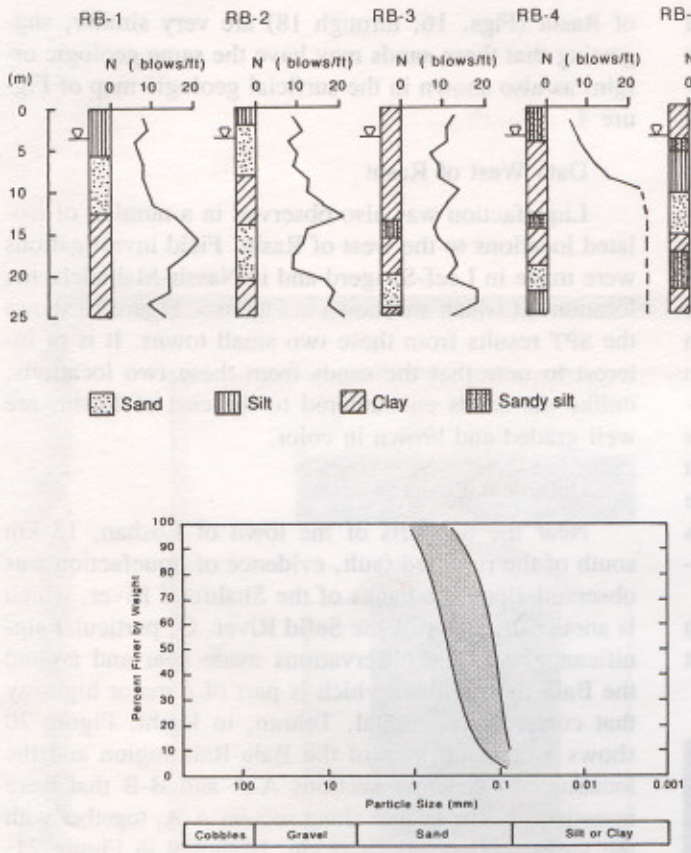

Figure 16. Borehole logs from Roudboneh and range of grain-size distribution.

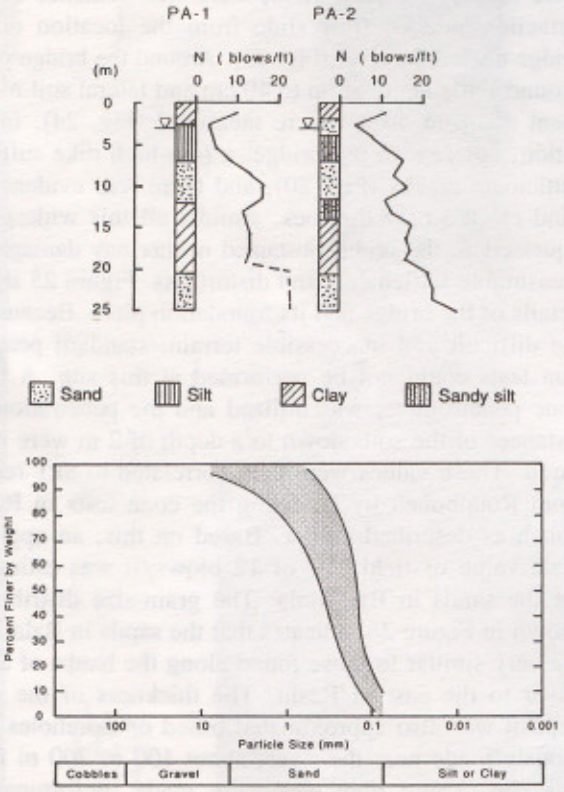

Figure 17. Borehole logs from Pahmedan and range of grain-size distribution.

a steel trestle founded on liquefied soil was investigated. Figure 20 shows the location of the trestle relative to the bridge. In Figure 27 a profile along section B-B is presented that describes the site conditions and observations made. Figure 28 shows a photo of the trestle with supports founded on 15-cm diameter steel pipe piles. Since most of the piles were embedded in the dense sandy gravelly river bed, no appreciable settlement of these piles was observed. Yet, liquefaction-induced ground settlements of up to 20 cm were observed and measured adjacent to the piles, as shown in Figure 29. The density of the sands at the trestle location was approximated in a similar manner as that for the bridge site, using hand cone penetrometer data.

In the companion article, the results of liquefaction and settlement analyses of these case histories are presented.

Summary

During the 1990 Manjil, Iran, earthquake, liquefaction and liquefaction-induced settlement of buildings contributed significantly to the devastation. Evidence of liquefaction was observed as far away as 85 km from the ruptured fault and near the Caspian Sea. The geologic map of the surficial soils in this region shows that liquefaction occurred primarily in the levee deposits along

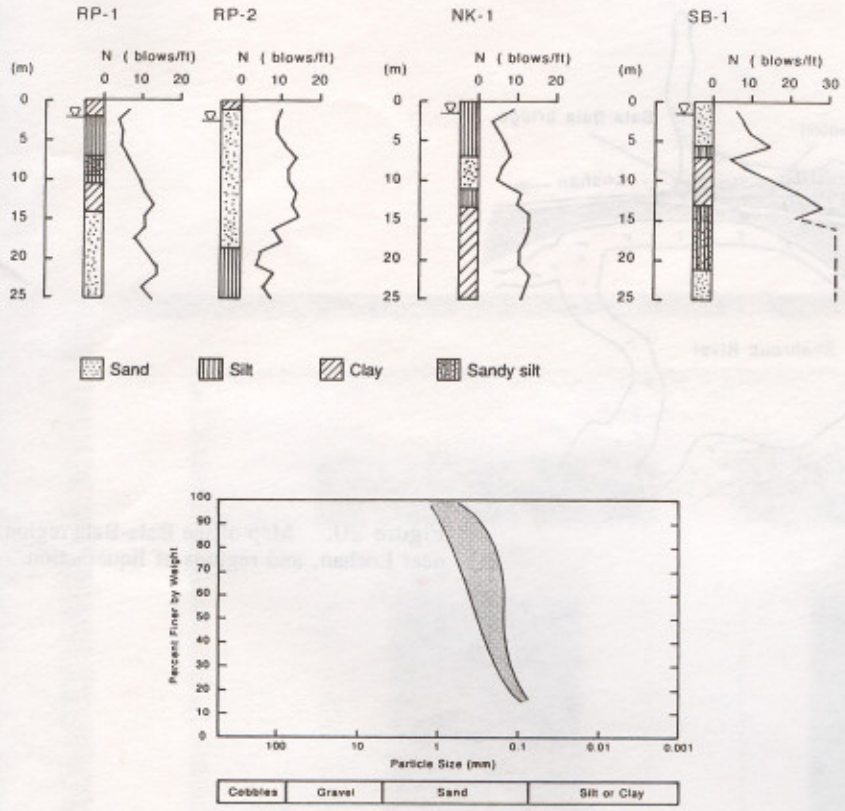

Figure 18. Borehole logs from Payin-Roudposht, Nasser-Kiadeh, and Safra-Basteh, and range of grain-size distribution.

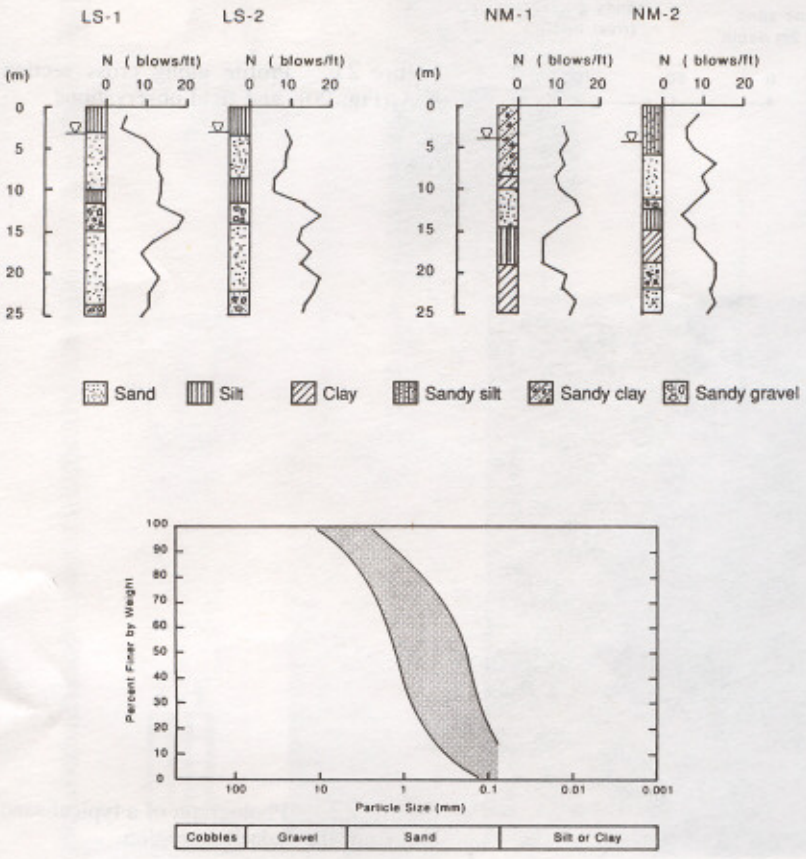

Figure 19. Borehole logs from Leef-Shagerd and Nassir-Mahalleh, and range of grain-size distribution.

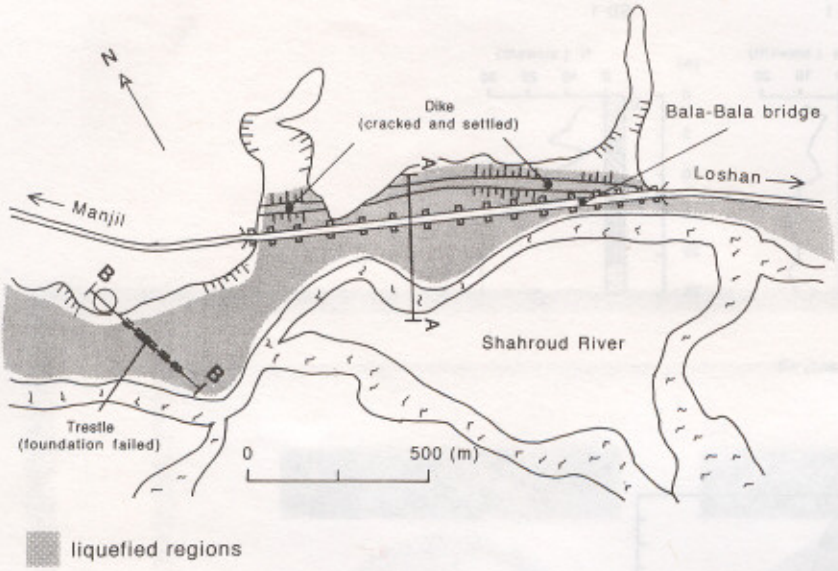

Figure 20. Map of the Bala-Bala region near Loshan, and regions of liquefaction.

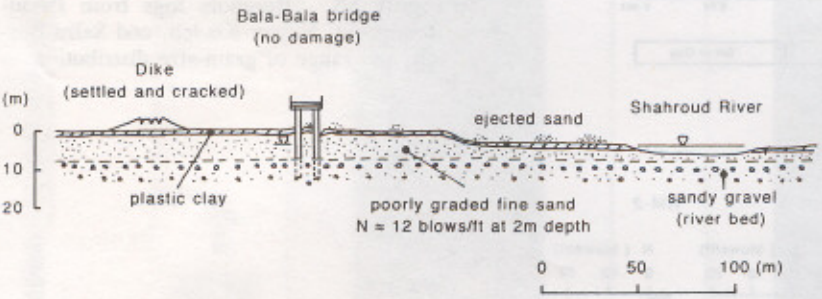

Figure 21. Profile along cross section A-A (Fig. 20), and field observations.

Figure 22. Photograph of a typical sand boil from the Bala-Bala region.

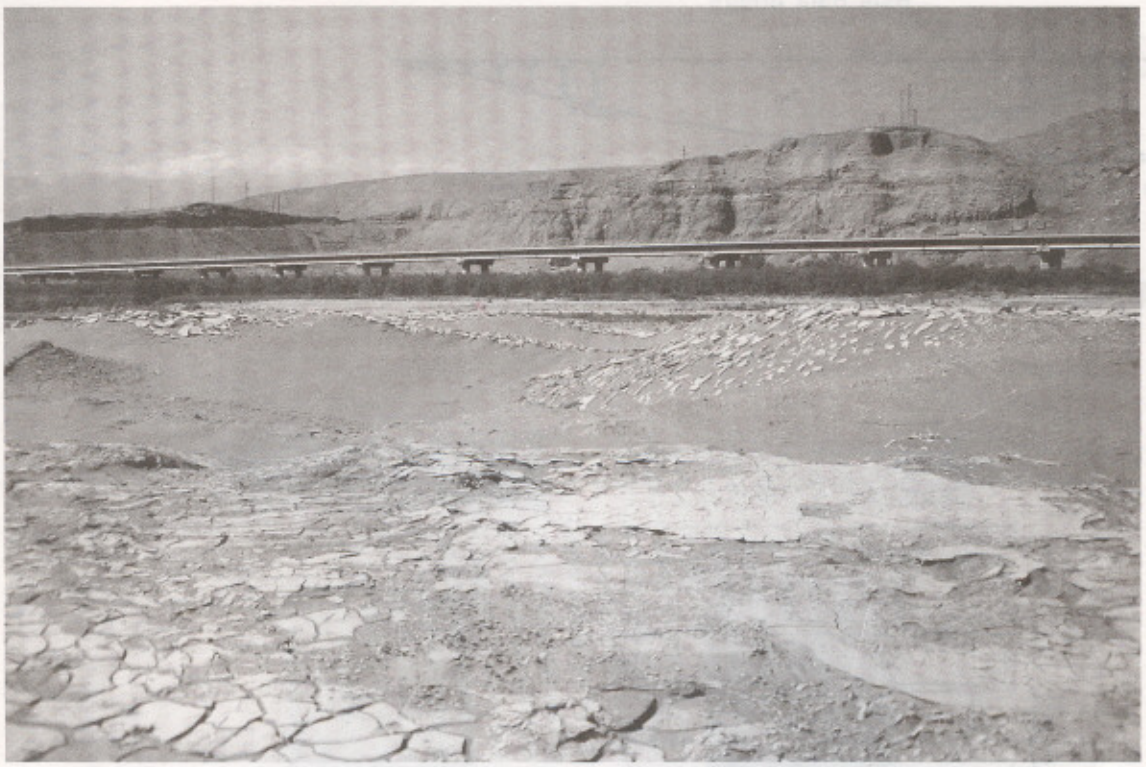

Figure 23. Photograph depicting liquefied sands that have laterally moved toward the Shahroud River.

Figure 24. Photograph showing settlement and permanent lateral displacement of the ground around the Bala-Bala bridge pier.

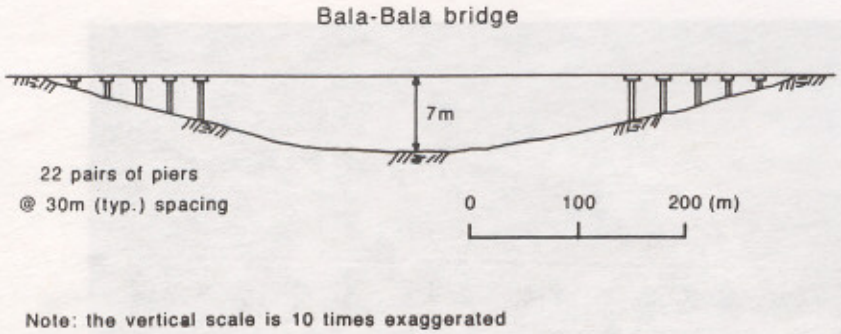

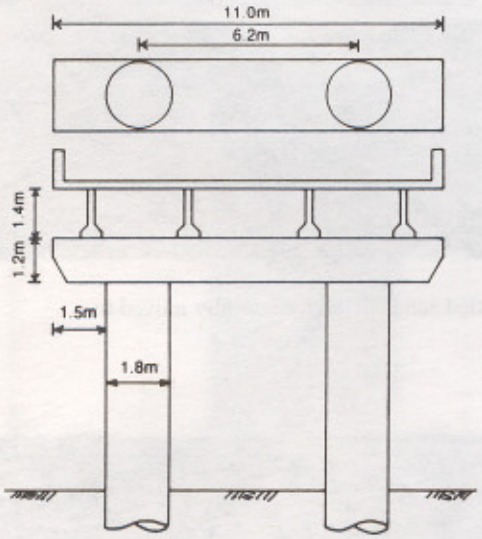

Figure 25. Details of the Bala-Bala bridge and its foundation piers.

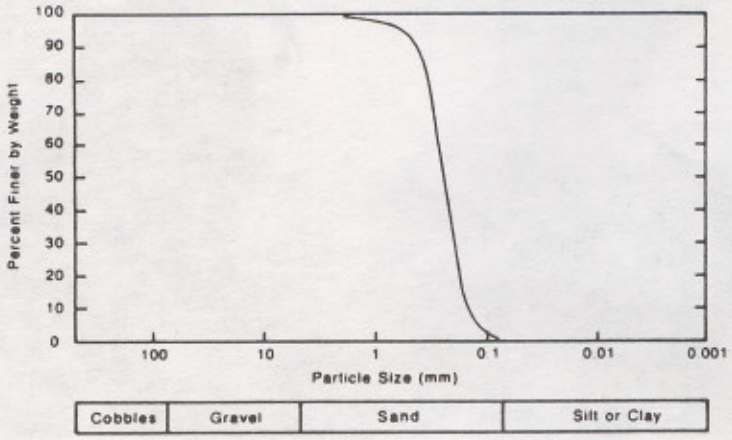

Figure 26. Grain-size distribution of the liquefied sands from the Bala-Bala region.

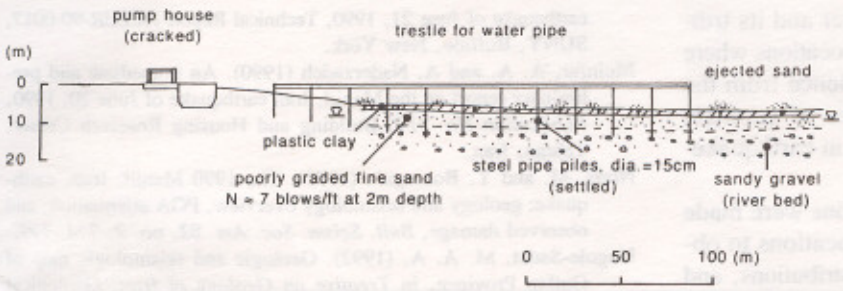

Figure 27. Profile along section B-B (Fig. 20), and field observations.

Figure 28. Photograph of a trestle founded on liquefied sand.

Figure 29. Photograph depicting ground settlement around the 15-cm-diameter pipe piles of the trestle.

the new and old channels of the Sefid River and its tributaries. Liquefaction also occurred in other locations where the sands are of marine origin. The experience from the Manjil earthquake suggests the importance of geologic input in mapping of liquefaction potential in earthquake-prone regions.

Extensive geotechnical field explorations were made 0in nine cities and towns at 33 different locations to obtain the geotechnical profiles, grain-size distributions, and densities of the liquefied and nonliquefied sands. This article presented the case history data useful for analyses of liquefaction, liquefaction-induced settlement of level ground and buildings, and permanent ground displacements. In a companion article, the results of the analyses of these data are presented.

Acknowledgments

Funding for the field surveys and geotechnical field investigations was provided by the Ministry of Housing and Urban Development of Iran, and the Office of the Governor of the Guilan Province. The authors gratefully acknowledge this support.

References

Astaneh, A. and M. Ghafori-Ashtiani (1990). The Manjil, Iran, earthquake of June 1990, *EERI Newsletter* **24**, no. 12.

Berberian, M., M. Qorashi, J. A. Jacksom, K. Priestley, and T. Wallace (1992). The Rudbar–Tarom 20 June 1990 earthquake in northwest Persia: preliminary field and seismological observations, and its tectonic significance, *Bull. Seism. Soc. Am.* **82**, no. 4, 1726–1755.

Haeri, S. M. and M. R. Zolfaghary (1992). On the earthquake induced liquefaction in Astaneh, Iran, *Proc. 10th WCEE*, Madrid, Spain, Vol. 1, A. A. Balkema Publishers, Rotterdam, Netherlands, 129–134.

Ishihara, K., S. M. Haeri, A. A. Moinfar, I. Towhata, and S. Tsujino (1992). Geotechnical Aspects of the June 21, 1990 Manjil earthquake in Iran, *Soils Foundations* **32**, no. 3, 61–78.

Mehrain, M. (1990). Reconnaissance report on the northern Iran earthquake of June 21, 1990, Technical Report NCEER-90-0017, SUNY, Buffalo, New York.

Moinfar, A. A. and A. Naderzadeh (1990). An immediate and preliminary report on the Manjil, Iran earthquake of June 20, 1990, *Publication No. 119*, Building and Housing Research Center, Tehran, Iran.

Niazi, M. and Y. Bozorgnia (1992). The 1990 Manjil, Iran, earthquake: geology and seismology overview, PGA attenuation, and observed damage, *Bull. Seism. Soc. Am.* **82**, no. 2, 774–799.

Nogole-Sadat, M. A. A. (1992). Geologic and seismologic map of Guilan Province, in *Treatise on Geology of Iran*, Geological Survey of Iran, Tehran.

Peng, K. Z. and P. Mozaffari (1990). The report of the near-field measurement on the aftershocks from the Rudbar, northwest Iran, earthquake on June 21st, 1990, Report No. 90-04, Beijing Strong-Motion Observation Center, Beijing, People's Republic of China.

Raifa, F., M. Shakarchi-Zadeh, H. Abd-Sharif Abadi, J. Farjoudi, and R. Mir-Ghaderi (1990). *Preliminary Evaluation of 31st Khordad 1369, and Its Effects on Guilan Province*, Housing Foundation of Islamic Republic of Iran, Tehran, Iran (in Farsi).

Shoaei, Z. and K. Sassa (1993). Mechanism of the landslides triggered by the 1990 Iran earthquake, *Bull. Disaster Prevention Res. Inst.* **43**, no. 1, Kyoto University, Kyoto, Japan, 1–29.

Yegian, M. K. and V. G. Ghahraman (1990). The Manjil, Iran, earthquake of June 1990, *EERI Newsletter* **24**, no. 12, 12–13.

Yegian, M. K., V. G. Ghahraman, M. A. A. Nogole-Sadat, and H. Daraie (1995). Liquefaction during the 1990 Manjil, Iran, earthquake, II: case history analyses, *Bull. Seism. Soc. Am.* **85**, no. 1, 83–92.

Department of Civil Engineering
Northeastern University
Boston, Massachusetts 02115
(M.K.Y. V.G.G.)

Geological Survey of Iran, and Department of Civil Engineering
University of Tehran
Tehran, Iran
(M.A.A.N.S.)

Consulting Geotechnical Engineer
Tehran, Iran
(H.D.)

Manuscript received 6 January 1994.